ASHESI UNIVERSITY

DESIGN AND FABRICATION OF AN INFLATABLE WING

CAPSTONE PROJECT

B.Sc. Mechanical Engineering

Dorcus Nakachwa

2019

ASHESI UNIVERSITY

DESIGN AND FABRICATION OF AN INFLATABLE WING

CAPSTONE PROJECT

Capstone Project submitted to the Department of Engineering, Ashesi University in partial fulfilment of the requirements for the award of Bachelor of Science degree in Mechanical Engineering.

Dorcus Nakachwa

2019

Declaration

I hereby declare that this capstone is the result of my own original work and that no part of it has been presented for another degree in this university or elsewhere.

Candidate's Signature:

……

Candidate's Name:

……

Date: ……

I hereby declare that preparation and presentation of this capstone were supervised in accordance with the guidelines on supervision of capstone laid down by Ashesi University.

Supervisor's Signature:

……

Supervisor's Name:

……

Date: ……

Acknowledgements

First and foremost, I wish to thank God Almighty for granting me the strength and ability to undertake this project. Without his blessings, this achievement would not have been possible.

I am thankful to my supervisor, Dr. Heather Beem whose encouragement and academic guidance helped me to accomplish this project.

I would also like to express my sincere gratitude to Nicholas Tali, Joseph Timpabi, Peter Lawerh and the entire staff and faculty of Ashesi's Engineering department. Their support and credible ideas have been great contributors in the completion of this project.

My acknowledgments would be incomplete without thanking my biggest support system, my family. I am grateful to my father; for always reminding me that I can do whatever thing I set my mind to, my mother; for her unflinching emotional support and to my siblings; for their love and care.

Abstract

This project paper explains the design and fabrication of an inflatable wing using a flexible, low cost and easily accessible PVC material. In recent times, several researchers have explored the building of inflatable structures using expensive and high strength materials like Mylar and Kevlar. However, this project scope was contextualized in the East African region where there is need for flexible and low cost Unmanned Aerial Vehicles (UAVs) for applications such as military surveillance. The project focused on using the NACA 4318 airfoil profile because it has a simple geometry that can easily be fabricated. PVC material was used to fabricate the wing because it is flexible, low cost, easily accessible and has a high tensile strength.

The wing was sewed, put together using epoxy and later heat sealed. After the wing was fabricated, static load tests and wind tunnel tests were performed on the wing. The wing was also simulated in a software, X – Foil where the lift and drag characteristics of the wing were predicted. The wind tunnel tests and X – Foil simulation showed that the stall angle of the wing was between 20° and 25°. In addition, the two data sets showed a trend as both the lift and drag coefficients increased and decreased with in the same range of angles of attack.

Key words: Inflatable structures, stall angle, lift and drag coefficient

Table of Contents

List of Figures

Chapter 1 : Introduction

More than a hundred years have passed since the first aircraft was launched into space. Several milestones have been attained in the aviation industry. For instance, Orville and Wilbur Wright built the first controlled and powered aircraft in 1903 [4]. Ever since, the industry has developed rapidly and one of the major developments recorded was the introduction of inflatable structures in aerospace applications. The use of inflatable structures was first deployed with the Echo I Mission in 1960 [1].

However, as more powerful launch vehicles became accessible, inflatable structures were abandoned. It was not until in the eighties and nineties that a renewed interest in inflatable structures yielded several projects for development and testing. The Inflatable Antenna Experiment (IAE) and the Inflatable Re-entry and Descent Technology (IRDT) program are some of the space flight tests that demonstrated the potential of inflatable structures. Since then, the technology has been highly sought for because inflatable structures allow for low storage volumes, they are low cost and lightweight and are easily deployable [11]. Therefore, this paper explains the design and fabrication of an inflatable wing for UAV applications.

1.1 Background and Motivation

Unmanned Aerial Vehicles (UAVs) have become an undeniable factor in both commercial and military arenas. Several departments of defense maintain a rigorous unmanned vehicles program. For instance, with in the United States Army, unmanned air and ground vehicles have been integrated into everything; from explosive ordinance disposal, to search and rescue [7]. In order to expand the applicability of UAVs, extensive and applied research has gone into making the technology more feasible, accessible and cost effective.

In this paper, the project was contextualized in the East African region. Thus, the inflatable wing was designed to be used in any of the East African countries. Worthy to note is that UAVs are not new to the East African people. In early 2018, Kenya legalized the commercial and private use of unmanned aerial vehicles [9]. Additionally, Kenya suggested the use of UAVs for military surveillance [9]. In other words, inflatable structures can be used for surveillance by East African troops in the ongoing Al Qaeda – Somalia conflict. The resources to build UAVs are very limited and therefore, this project suggests how East African counties can build UAVs using inflatable wings. The inflatable wings will reduce the cost of building the UAVs as the wings were made from the cheap and easily accessible PVC material.

1.2 Hypothesis

Inflatable wings can be fabricated from cheap and readily available materials from Africa and their performance is comparable (regarding flow characteristics like lift and drag) to that of the rigid wings currently being used.

1.3 Objectives

In this project, the major objectives are:

- To design and build an inflatable wing
- To test and discuss pertinent parameters related to the wing. For instance, the wing would be tested on static and dynamic loading properties for instance lift and drag. The results derived from these tests would be explained in detail.
- To provide enough information on the wing configuration regarding the design and structural properties so that the data in this project may be extrapolated to other cases in the future.

1.4 Success Criteria

Success would be attained when test parameters such as lift and drag, under the repeated performance of the inflatable wing is reliable with reference to scientific reasoning; specifically, in the field of fluid mechanics.

1.5 Strategy and Value to Technical Community

Regarding the value to technical community, this project used a cheap and readily available material to fabricate an inflatable wing.

Chapter 2 : Literature Review

2.1 Overview

Over the years, there have been several innovations to make space vehicles fly. From fixed wings to rotary and oscillating wings [13], these inventions have improved the overall aircraft efficiency. In addition, several lighter – than – air vehicles for example balloons and blimps have been devised but they require a larger volume of air or helium during the inflation process [7]. One of the recent innovations in aviation are inflatable wings. Inflatable wings are considered a safer option because they require much less air or helium and could also be blown up by mouth within 2 – 3 minutes. Inflatable wings also take up less volume by rolling up firmly and would also weigh much less. Therefore, in this chapter, different designs of inflatable wings that have been developed by researchers are explained.

2.2 Previous work

Four papers were reviewed, forming part of the research undertaken during this project. The first paper [6], was assigned by the United States of America as represented by the United Sates Department of Energy, Washington, D.C. In the paper, Priddy designed and built an inflatable wing, which was formed from a pair of tapered, conical inflatable tubes that were in tangential contact with each other. Each airfoil had at least two air – tight inflatable tubes, which were made from Mylar. The tubes were further bound together using top and bottom reinforcement boards; the boards were made of a reinforcement material called Kevlar.

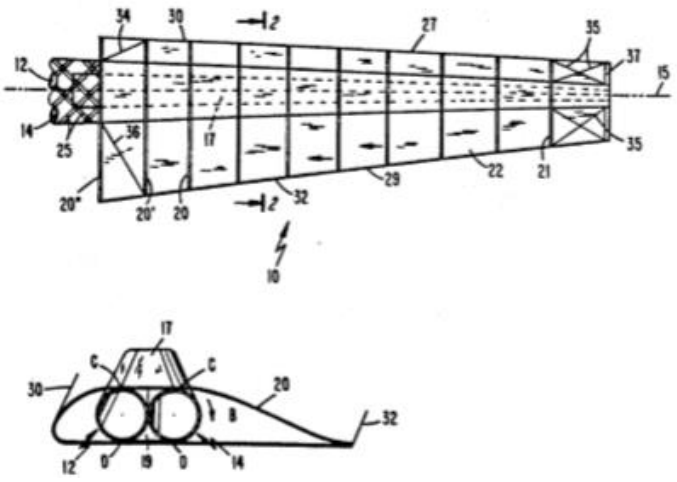

Figure 2.1: The top and side views of the inflatable tubes of the wing and the top – down reinforcement [6, Fig. 1]

The reinforcement method proposed by Priddy may have some undesirable characteristics when building a light weight inflatable wing. The author used Kevlar to perform a top – down reinforcement for the wing. Kevlar is a heat – resistant and strong fiber and it is usually used to make bullet proofs. Although the material has great material properties, it is not light-weight and making it a reinforcement added weight to the already Mylar-made wing. Instead of Kevlar, a better option was carbon fiber, which has a high ultimate strength and is extremely light. However, the use of air tight inflatable tubes by the author was a recommendable option as it is easy to implement.

In the second paper [2], Lebeau and Jacob present two aspects for current development efforts of inflatable wings for Mars exploration that is: low-altitude flight testing of an inflatable-wing aircraft and computational fluid dynamics (CFD) simulations of different wing geometries.

In their paper, the authors used the NACA 4318 and Eppler 398 airfoils. For both airfoils, bumpy and smooth wing samples were built and tested across a range of conditions including weather and payload. Performance characteristics like stall velocity and endurance were also

included in the flight tests. The CFD and experimental results suggested less flow separation for bumpy profiles as compared to the smooth ones. The results also suggested that the presence of bumps on the airfoil significantly reduced the dynamic pressures on a wing, resulting in a loss of lift.

Figure 2.2: The smooth (left) and bumpy (right) airfoil profiles for NACA 4318 [2, Fig. 22]

For the third article [3], David et al discuss the efforts of reshaping or morphing of an inflatable wing to provide roll control through warping. The authors also used the NACA 4318 airfoil profile and the surface of the airfoil was bumpy making the wing appear as a series of interconnecting cylinders. Bumps have a positive effect on wing performance at low Reynolds numbers and help to maintain flow attachment. The Reynolds number is a dimensionless number used to determine whether fluid flow over an object is laminar or turbulent.

However, at high Reynold numbers, a smooth fabric was added to the surface of the wing to reduce aerodynamic drag. The material used to manufacture the wing was Vectran, a high strength liquid crystalline polymer with excellent mechanical properties for UAV wings. The morphing capability of the wing was developed depending on the wing's internal structural and inflation loads. In the project, morphing was achieved by using a technique called 'bump flattering,' where actuators were applied directly to the wing restraint. The authors developed considerable data for the design of a morphing inflatable wing. The concepts derived had a

significant contribution to the manufacture of inflatable wings for small UAVs and may also be applied for aspect ratio morphing of larger UAVs.

It was noted in the second paper [2] as well as in the third paper [3] that a bumpy profile of the wing was adopted. According to the article by Bari et al [10] this was a safe option. This is because flow separation on the airfoil can be delayed by using bumps on the upper surface of the airfoil [10]. However, the use of actuators to inflate the wing in the third article might have added more weight to the aircraft and this could have altered the flight test data recorded.

Lastly, the fourth paper [7] presented as a thesis by Brown, explains a simulation model and an experimental platform, which was designed to gain quantitative and qualitative understanding of the unique characteristics of an inflatable wing. In the paper, Brown designed and built a suitable platform for capturing flight test data. He also built an inflatable wing model, which he tested and collected data on. In the project, the author found the built model to be capable of making a perfect match to the flight tests data. Thus, the model was an adequate baseline for future platforms and other aerodynamic surfaces.

In the fourth paper [7], the decision to use air to inflate the wing was a better option. This is because air is readily available, and this made the procedure easy to deploy. Additionally, the use of air does not add excess weight to the inflatable wing.

2.3 Summary

To a large extent, all the previous research and proposed models address the dynamics of how inflatable wings operate. Several models deployed the NACA 4318, which is a common airfoil profile used in the aerospace industry. Some of the materials proposed in the papers are not light weight and are not readily available. Additionally, the methods of inflating the wing were also undesirable as they add excess weight to the structure. Therefore, more research is needed into finding a cheap and readily available material to fabricate inflatable wings. In addition, the use of air should be explored as the best option of inflating the wings. This is because air is readily available from the environment.

Chapter 3 : Design

3.1 Overview

This chapter explains how the inflatable wing was fabricated. It describes the materials and tools that were used to build the wing. Also, it explains the tests that were designed to be carried out on the wing.

3.2 Technical Approach

The first major decision undertaken on this project was the material selection. The design options were Kevlar, Hypalon, PVC, Neoprene and Urethane as they are the most commonly used materials used to build inflatable structures as suggested from the literature review. These design options were further analyzed using the Pugh matrix to determine the most suitable material. With the matrix, the evaluation criteria were availability, cost, strength and manufacturability (in order of priority) because the project was aimed at using a readily available material to fabricate an inflatable wing. After the evaluation, it was observed that PVC (as shown in figure 3.1) was the best material to build the wing. As specified in table 3.1, PVC scores 8, which is the highest score on the Pugh matrix.

Table 3.1: A table showing the evaluation of the design material options

Evaluation Criteria	Weight	Baseline	Kevlar	Hypalon	PVC	Neoprene	Urethane
Availability	4	0	-4	+3	+4	+2	+2
Cost	3	0	-3	+2	+3	-3	-3
Strength	2	0	+2	+1	0	+1	+1
Manufacturability	1	0	-1	+1	+1	-1	-1
Total			-6	7	8	-1	-1

Figure 3.1: The PVC material, which was used to build the wing

The next step was to design both the airfoil cross section and the wing that were to be used during fabrication. This was achieved using SolidWorks. The two designs informed the entire fabrication process. From the literature review, it was observed that the NACA 4318 was the most frequently used airfoil profile because it is easily deployable, and it generates a desirable lift force. Therefore, for this project, the NACA 4318 airfoil profile was used as seen in figure 3.2 and the wing design in figure 3.3. The airfoil measured 24 centimeters of chord length and the span was 26 centimeters.

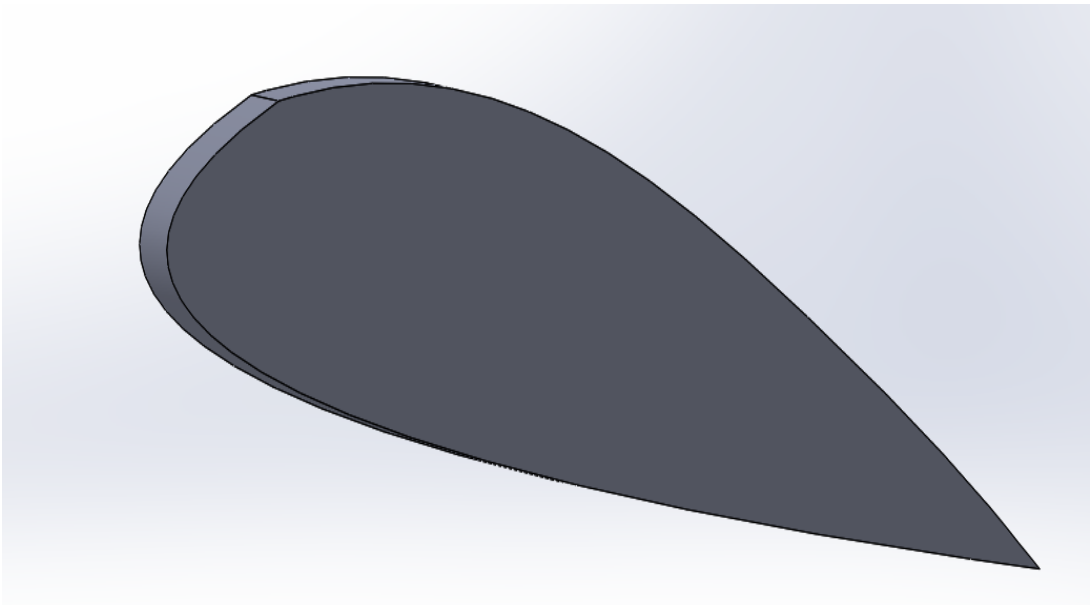

Figure 3.2: The NACA 4318 profile as designed in SolidWorks

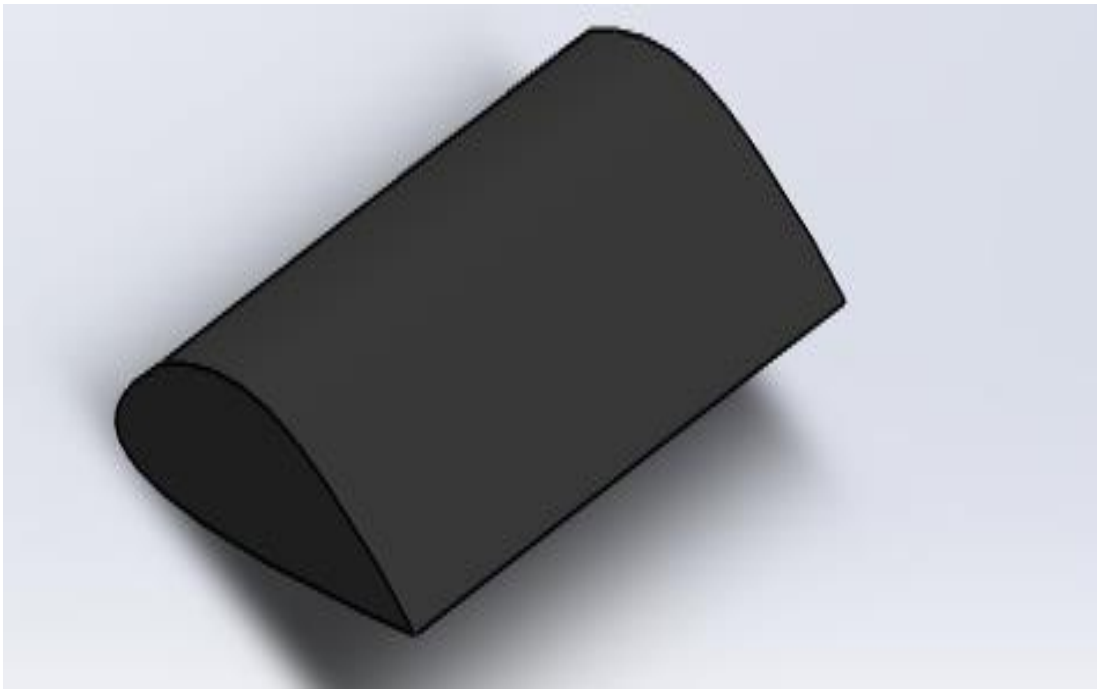

Figure 3.3: The design of the inflatable wing in SolidWorks

3.3 Experimental Design

Several tests were designed to be conducted in this project. Tests to evaluate flow properties of the wing were designed to be conducted on the wing. The static and dynamic loading tests are explained in detail below:

1. Static loading

Static load tests were performed on the inflatable wing. The wing was rigidly secured in the center section while the wing tips were being loaded. Loads amounting to a total weight of 5000grams were placed on the wing. An infra-red motion sensor (as shown in figure 3.4) was used to measure the displacement. The motion sensor was connected to a Lab quest where the displacement was read off directly.

Figure 3.4: The static load test being carried out

2. Dynamic loading

The dynamic loading tests were carried out in a wind tunnel. The main goal of the dynamic testing was to establish the lift and drag properties of the wing as illustrated in figure 3.5.

Figure 3.5: The dynamic loading tests being carried out in a wind tunnel

Chapter 4 : Implementation

4.1 Overview

In this chapter, the fabrication process will be explained in detail. Overall, four prototypes were built before the desired wing design was achieved. For the fabrication, the PVC material was cut into appropriate pieces that fit the design of the suggested airfoil and wing. These pieces were glued together using epoxy to form the wing. The seams of the wing were heat sealed to create a more air – tight structure. A compressor was used to inflate the wing with air because air is readily available in the atmosphere.

Figure 4.1: The epoxy that was used to glue the PVC material

In order to maintain a neat air foil cross section throughout the project, an already existing NACA 4318 profile was obtained online [14] and it was printed and glued onto cardboard. This became the air foil paper template used to fabricate all wing prototypes.

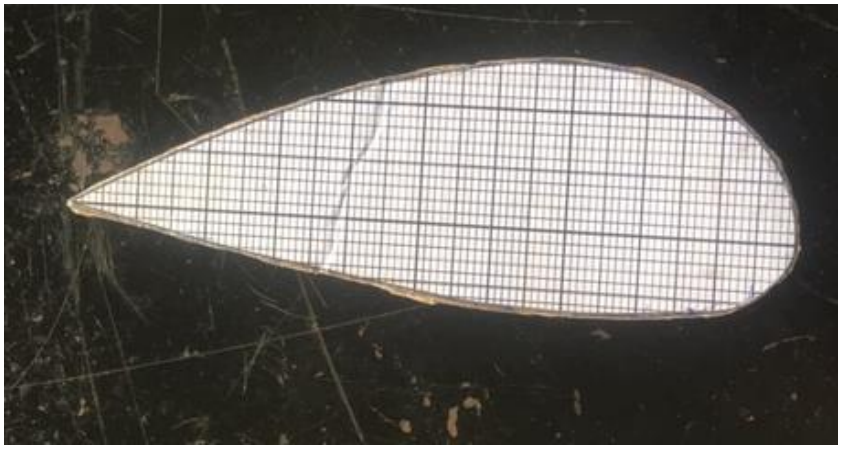

Figure 4.2: The NACA 4318 paper template that was used in the project

4.1 Prototype 1

In order to fabricate the first prototype, Nylon material was used as the starting material because the PVC material had not been purchased at that time. The nylon material was used to build the first and second prototypes.

Figure 4.3: The nylon material used to make the first and second prototypes

Regarding the first prototype, the wing had smooth edges, but the airfoil cross-section was not clearly outlined.

Figure 4.4: Prototype 1 with smooth edges but no clear airfoil cross section

4.2 Prototype 2

With the first prototype having no clear cross section, there was need to build a second prototype that had a clear airfoil cross section. In the second prototype, a clear airfoil cross-section was achieved by gluing the air foils on the outside as opposed to the first prototype where the airfoils were glued on the inside. However, the wing edges of the second prototype were not smooth as shown in figure 4.5.

Figure 4.5: Prototype 2 with a clear airfoil cross section but the edges are not smooth

4.3 Prototype 3

From figures 4.4 and 4.5 it was observed that there was a compromise between having a clear airfoil cross-section and smooth wing edges. Thus, a new fabrication method was developed. The material was sewed to give the desired airfoil cross section while also maintaining the smooth edges. At this point, the PVC material had been purchased and it was used in the next prototypes.

Figure 4.6: The sewed material giving a clear airfoil cross section

Figure 4.7: The sewed wing

4.4 Prototype 4

Although sewing produced a smooth-edged wing with a clear airfoil cross section, it was not enough to make the wing air - tight. Therefore, the seams of the wing were attached together using epoxy and they were heat sealed (as shown in figure 4.9) afterward to make the wing air - tight.

Figure 4.8: The inside seams of the wing attached together with epoxy

Figure 4.9: The inside seams being heat sealed to make the wing air tight

Figure 4.10: The heat-sealed seams of the wing

Note that the wing was sewed from the inside. The inside seams were joined together using epoxy and later heat sealed (as in figure 4.10) to make the wing air tight. The wing was later turned over and the desired outside part was obtained. The outside seams were also joined together with epoxy and heat sealed and the final inflatable wing was developed (figure 4.11).

Figure 4.11: The final smooth-edged wing with an elaborate airfoil cross section

Worthy to note is that at the start of the project, the scope was to fabricate an automatically inflating wing. One side of the wing would be attached to the body of the aircraft while the other would be rolled up. During takeoff of the aircraft, the wing would inflate automatically to form a full-outstretched structure. However due to limited resources, the wing was not made to be self-inflating. Figure 4.12 shows how the wing would be rolled up.

Figure 4.12: An illustration of how the wing would be rolled up

Chapter 5 : Testing and Results

5.1 Overview

Experiments were designed to test the performance of the inflatable wing. These experiments examined static and dynamic properties of the wing. Lift and drag characteristics of the wing were derived from the wind tunnel test. However, design predictions were made using a simulation software called 'X – Foil.' X – Foil is an interactive software for the design and analysis of isolated airfoils. With a specified set of coordinates describing the shape of a 2D airfoil and Reynolds number, the software can generate the pressure distribution on the airfoil and the lift and drag characteristics. X-Foil results were run in MATLAB and an analysis was performed on both the simulation and wind tunnel results.

5.2 Results from the simulation tests in X-Foil

As shown in figure 4.2, the airfoil used in this project was the NACA 4318. Thus, the NACA 4318 profile was used to generate lift and drag characteristics in X – Foil. The Reynolds number that was used during the simulation was derived from the formula:

Reynolds number, $Re = \frac{\rho u L}{\mu}$

ρ is the density of air (SI units: kg/m^3)

u is the velocity of air with respect to the object (m/s)

L is a characteristic linear dimension (m)

μ is the dynamic viscosity of air (Pa·s or $N \cdot s/m^2$ or kg/m·s)

With a wind speed of $8ms^{-1}$, and a characteristic length of 26cm, the Reynolds number used was:

Reynolds number, $Re = \frac{26*10^{-2}*8}{1.5*10^{-5}} = 138.6667 * 10^3$. This Reynolds number was maintained for all experiments.

From X – Foil, the values of angle of attack, lift coefficient and drag coefficient were obtained in a csv file and later plotted in MATLAB as shown in figure 5.1.

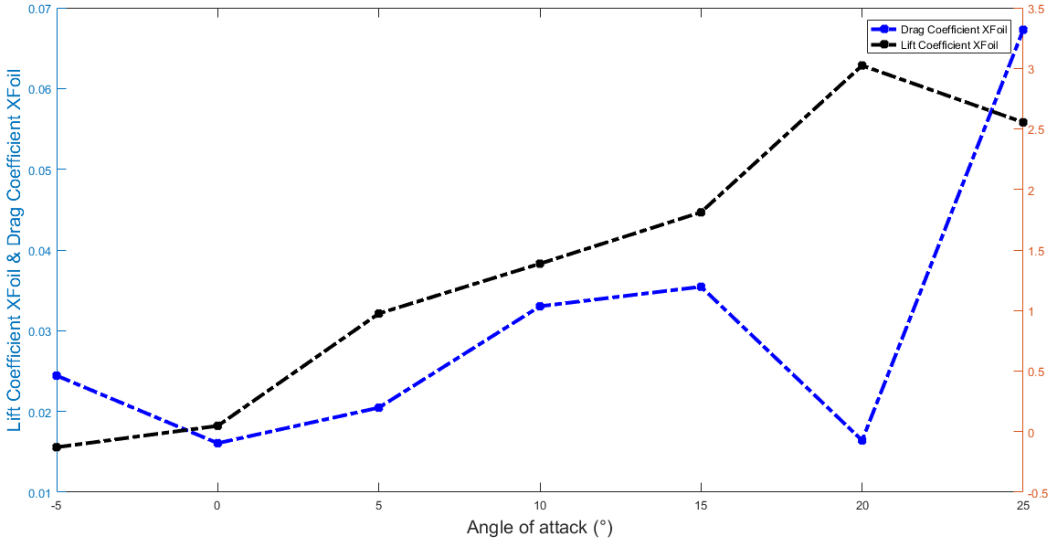

*Figure 5.1: The graph of lift and drag coefficient against angle attack as generated by X Foil at a Reynolds number of 〖138.6667*10〗^3*

From figure 5.1, the lift coefficient increased from -5° to 20° and it decreased between 20° and 25°. The period through which the lift coefficient decreased is called stalling. The angle of attack at which the lift coefficient started to decrease is called the stall angle. From figure 5.1, the stall angle is predicted to be between 20° and 25°. It is important to know the stall angle of the wing because it helps pilots to stop the aircraft from losing lift during flight.

Still on figure 5.1, the drag coefficient decreased between angles of attack -5° and 0°. After that, the drag coefficient increased steadily. At 20°, the drag coefficient was supposed to increase but it decreased and thus, this point is considered as an outlier.

5.3 Results from the static load tests

The main purpose of static load tests was to show the bending and structural properties of the wing. If the wing does not go through permanent deformation after the loads have been placed on it, then the wing is said to be strong. In this project, loads of 500g (up to 5000g) were placed subsequently on the wing and the respective deflection was measured. A graph of deflection against load was derived in Microsoft Excel.

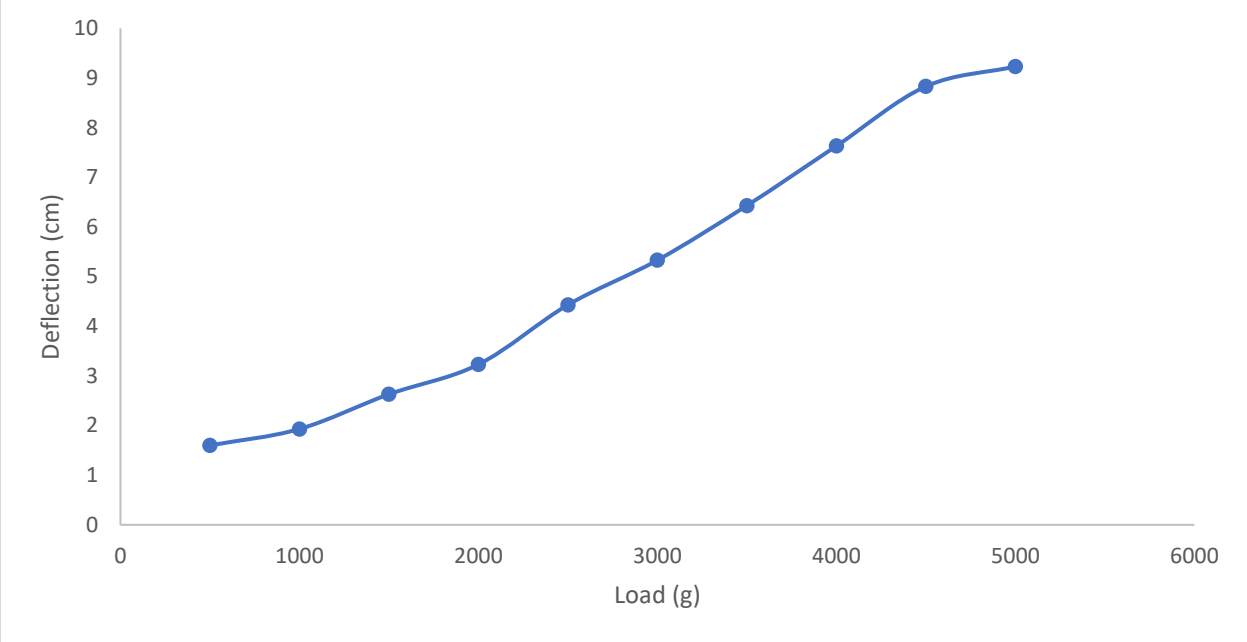

Figure 5.2: The graph of deflection against load

From figure 5.2, the deflection of the wing increases as more loads are placed on it. However, when the loads are released from the wing. It does not experience plastic deformation as it slightly comes back to its initial position. The wing experienced a maximum deflection of 9.23 cm and it returned to the 0.89cm mark just below the zero line.

5.4 Results from the wind tunnel tests

The wind tunnel tests were aimed at examining the lift and drag characteristics of the wing. The wing was hooked horizontally in the test section of the wind tunnel. With the fan switched on, lift and drag data was collected on the wing at angle of attack of 0° and with varied wind speeds. The major reason as to why the wing was tested at varied wind speeds was because there was need to establish a stable wind speed at which all experiments would be conducted.

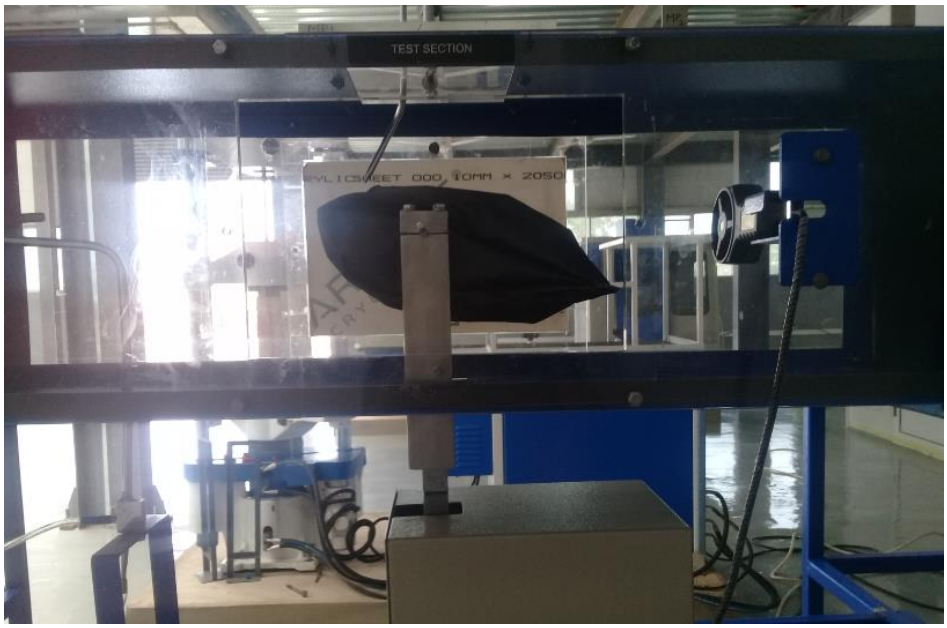

Figure 5.3: The wing placed in the test section of the wind tunnel

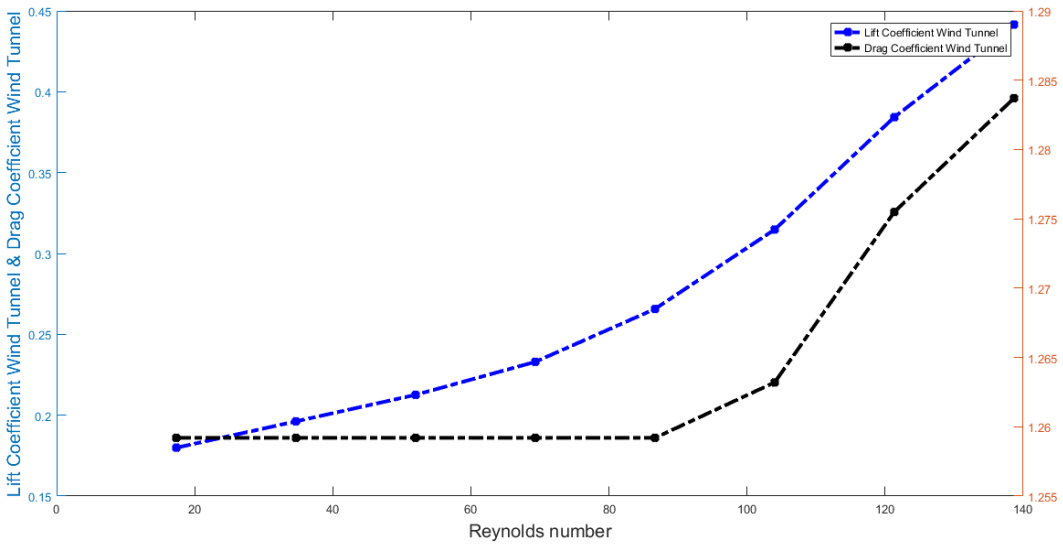

Figure 5.4: The graph of lift and Drag Coefficient against varied Reynolds Numbers

As seen in figure 5.4, the lift coefficient was constant from a Reynolds number of $17.3333 * 10^3$ to $86.6667 * 10^3$ and in terms of wind speed, it was $1ms^{-1}$ to $5ms^{-1}$. The lift coefficient only started to increase at a Reynolds number of $104 * 10^3$ (wind speed of $6ms^{-1}$). The drag coefficient on the other hand increased steadily throughout the graph. This test established that a Reynolds number of $138.6667 * 10^3$ (wind speed of $8ms^{-1}$) was a more stable value to conduct all experiments.

After a stable Reynolds number of $138.6667 * 10^3$ (wind speed of $8ms^{-1}$) was established, lift and drag data was obtained at varied angles of attack (from -5° to 25° at an interval of 5°) as explained in figure 5.5.

However, the data collected from the wind tunnel was lift and drag force. Thus, there was need to obtain dimensionless values by calculating the lift and drag coefficients from the formulas below.

The lift coefficient was calculated from

$$C_L = \frac{2 * L}{\rho * V^2 * A}$$

Where:

L is the lift force

ρ is the density of air, which is known as $1.225 kg/m^3$

V is the wind speed, which was $8 ms^{-1}$

A is the wing area; the wing was 26cm by 24cm

C_L is the coefficient of lift

The coefficient of drag was derived using the same formula, which is

$$C_D = \frac{2 * D}{\rho * V^2 * A}$$

Where:

D is the drag force

ρ is the density of air, which is known as $1.225 kg/m^3$

V is the wind speed, which was $8 ms^{-1}$

A is the wing area; the wing was 26cm by 24cm

C_D is the coefficient of lift

The lift and drag coefficients were derived for all the lift and drag values obtained from the wind tunnel test and these were plotted in MATLAB as shown in figures 5.5, 5.6 and 5.7.

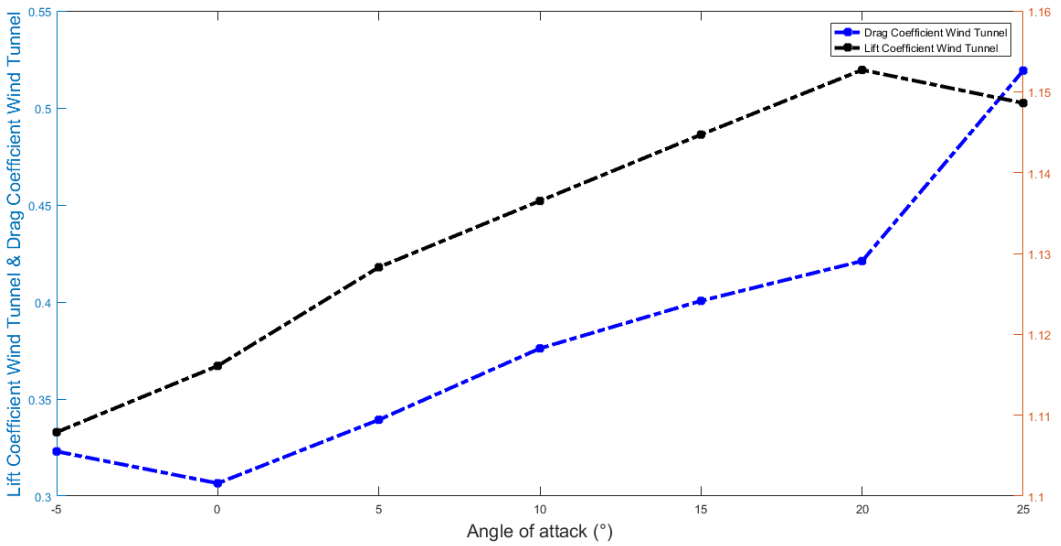

Figure 5.5: The graph of lift and drag coefficient against angle attack as read from the Wind Tunnel at a Reynolds number of $138.6667 * 10^3$

From figure 5.5, at a Reynolds number of $138.6667 * 10^3$, the lift coefficient increased from -5° to 20° and it decreased between 20° and 25°. The condition through which the lift coefficient decreased is called stalling. The angle of attack at which the lift coefficient started to decrease is called the stall angle. From the graph, the stall angle was predicted to be between 20° and 25°. On the other hand, the drag coefficient decreased between angles of attack -5° and 0°. After that, the drag coefficient increased exponentially.

After all the experimental data was gathered, there was need to analyze the two data sets. Thus, the lift coefficients from both X – Foil and the wind tunnel were plotted on the same graph as shown in figure 5.6.

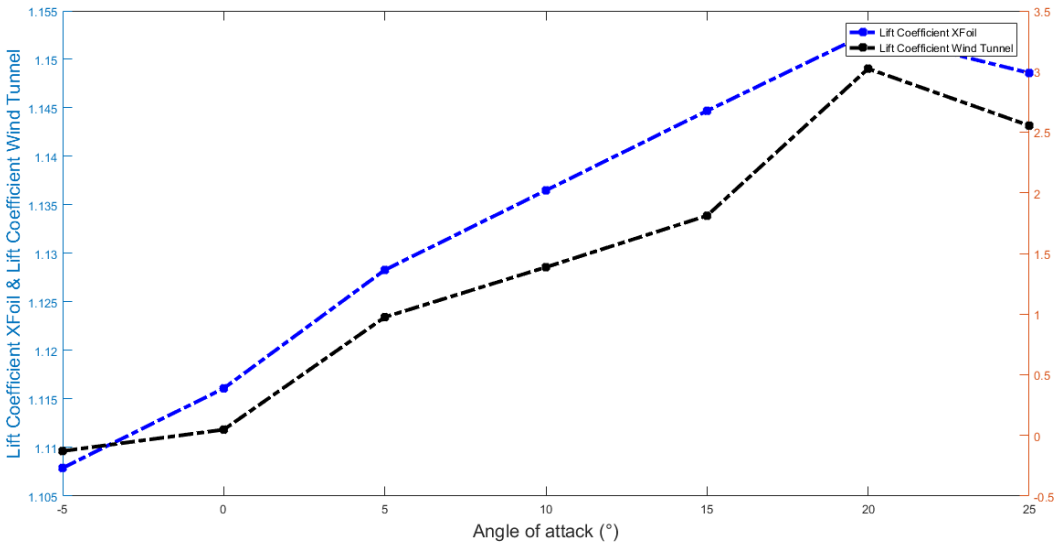

Figure 5.6: The graph of lift coefficients from both X Foil and the wind tunnel against angle attack at a Reynolds number of $138.6667 * 10^3$

From figure 5.6, a trend was observed between the lift coefficient from X – Foil and the wind tunnel. The data from the two experiments increased and decreased with in the same range of angles of attack. For instance, the two lift coefficient data sets increased from -5° to 20° and decreased between 20° and 25°. From this observation, it was established that the stall angle of the airfoil in this project was between 20° and 25°.

Although the lift coefficient from the Wind tunnel was higher than that of X – Foil in the beginning, the lift coefficient from X – Foil stayed significantly bigger than that of the wind tunnel after about -4°. The highest value of the lift coefficient obtained from X – Foil was 3.0236 whereas that of the wind tunnel was 1.1527. Thus, the difference between the two peaks was 1.8709. The wind tunnel lift was lower than that of X – Foil because of:

1. Loss of flow due to the low aspect ratio of the fabricated wing.

The aspect ratio of a wing as described by Harbig, Sheridan and Thompson in their paper [12] is the ratio of the wing's span to its mean chord length. In the wind tunnel tests, the wing

used had a chord length of 24cm and its span was 26cm. Therefore, the aspect ratio (AR) of the wing was:

$$\text{Aspect ratio (AR)} = \frac{26}{24} = 1.08$$

As explained in the article [12] by Harbig et al, low aspect ratios (less than 3) usually lead to a loss of flow by the wing. The loss of flow also ends up in the loss of lift. Thus, it was not surprising to observe low lift coefficients from the wind tunnel because the aspect ratio of the wing tested was 1.08, which is a low value since it is less than 3.

2. Rough edges of the wing

The inflatable wing that was used during the wind tunnel tests did not have perfectly smooth edges. Therefore, vortex wakes were created around the edges of the wing and leading to a loss in fluid flow, which eventually caused a loss in lift. This describes why the lift coefficient from the wind tunnel was lower than the lift coefficient from X – Foil.

3. Equipment and sensor errors

The difference between the lift coefficients of X – Foil and the wind tunnel was caused by equipment and sensor errors from the wind tunnel. The errors lowered the lift obtained from the wind tunnel.

With the lift coefficients compared and analyzed, it was inevitable that the drag coefficients from X – Foil and the wind tunnel be compared as well. The results are summarized in figure 5.7.

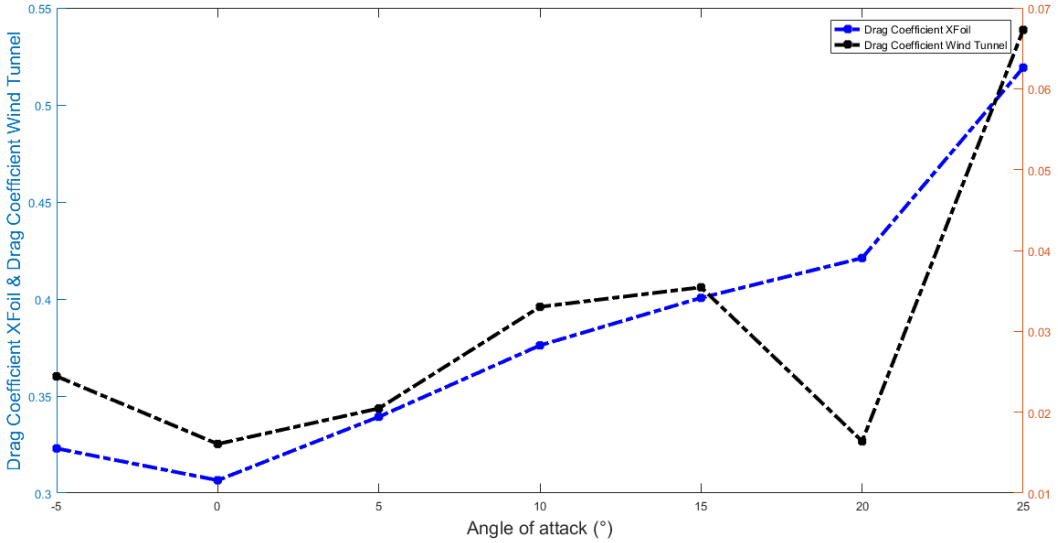

Figure 5.7: The graph of drag coefficients from both X Foil and the wind tunnel against angle attack at a Reynolds number of $138.6667 * 10^3$

From figure 5.7, the drag coefficient from the wind tunnel was considerably higher than that from X – Foil. As described from figure 5.6, when the lift coefficient from the wind tunnel decreases, the drag coefficient was expected to increase as seen in figure 5.7.

5.5 Experimental errors and error mitigation

The most significant source of error that could have occurred in the experiment was the variability in the geometry of the airfoil. Human errors in measuring, cutting and gluing the wing together may also have altered the geometry. These errors were mitigated by having an already cut out airfoil cross section, which was traced on the material. The traced-out part was then used to build the airfoil. Additionally, several prototypes of the airfoil were fabricated until the perfect airfoil shape was attained.

Chapter 6 : Conclusion

In this chapter, qualitative conclusions will be made on the results derived in the experiments conducted in this project. In addition, the chapter will explain the limitations encountered during the execution of the project. Recommendations will also be suggested for future work of the project.

6.1 Discussion

The results obtained in the static load tests showed that the material used to fabricate the wing had strong structural properties. This is because the wing did not permanently deform as it recovered from a 9.23 cm deformation to a 0.89 cm mark just below the zero line. Regarding the X – Foil simulation and the wind tunnel tests, the results showed that the stall angle of the fabricated wing was between 20° and 25°. This was the case for results from the X – Foil simulation and the wind tunnel tests.

However, the lift coefficient from X – Foil was higher than that of the wind tunnel tests. The drag coefficient from X – Foil was lower than that of the wind tunnel tests on the other hand. The variation between the two data sets was caused by the low aspect ratio of the wing used in the wind tunnel tests as this led to a loss in flow and eventually caused a loss in lift. Rough edges of the wing and equipment errors of the wind tunnel sensors were also a major contribution to the low lift coefficients obtained from the wind tunnel. Both X – Foil simulation and the wind tunnel results showed a trend as the stall angle was between the same range and the lift and drag coefficients increased and decreased with in the same range of angles of attack.

Ultimately, although there were some experimental errors that were associated with this project, the results from the testing and results chapter show that the use of inflatable wings on UAVs is a reliable and valid technology that can further be explored. This project established that East African countries can use the low cost and readily available PVC material to fabricate inflatable winged UAVs that can be used for several applications for instance military surveillance.

6.2 Limitations

In this project, the major limitation was making the inflatable wing air - tight. The use of epoxy by itself could not make the wing air - tight. This is because epoxy left small pores on the outline of the wing where air could escape. Therefore, heat sealing the seams of the wing created a continuous airtight layer where air could not escape.

Another limitation was getting the exact profile of NACA 4318. As seen in figures 4.2 and 4.3, it was quite difficult to get smooth wing edges and a clear profile by using epoxy only. The introduction of sewing as a fabrication method made the whole process easy.

6.3 Future Work

In future work, it would be useful to have an actual Unmanned Aerial Vehicle (UAV) where the inflatable wings would be tested. This is because the UAV would give the real depiction of how the inflatable wing would work.

Additionally, for future work, it is proposed that a self – inflating wing system is built. It would also be worthwhile to have the wings attached to the UAV. This would give a more robust picture of how the inflatable winged UAV would perform. Also, it would show how the wings would inflate during takeoff and collapse after landing. It would also be of interest to demonstrate how the UAV would carry out military surveillance. This could be done at different angles.

Lastly, the aerodynamic performance of the inflatable wing configured in this research could also spark interest in the exploration of alternative wing designs. As noted in this paper, the wing design used has a smooth profile. Thus, in future work, a bumpy wing profile could be used to fabricate the inflatable wing. This is because bumpy profiles allow maximum flow attachment of the wing [2].

References

[1] T.-M. TOMESCU, "Buletinul AGIR," 1 January 2010. [Online]. Available: www.agir.ro/buletine/685.pdf. [Accessed 27 September 2018].

[2] D. A. Reasor, J. D. Jacob, R. P. LeBeau and S. W. Smith, "Flight Testing and Simulation of a Mars Aircraft Design Using Inflatable Wings," *American Institute of Aeronautics and Astronautics,* vol. 6, no. 2, pp. 1-24, 2007.

[3] D. Cadogan, T. Smith, F. Uhelsky and M. MacKusick, "Morphing Inflatable Wing Development for Compact Package Unmanned Aerial Vehicles," *American Institute of Aeronautics and Astronautics* , vol. n.a, no. n.a, pp. 1-13, 2004.

[4] M. Salama, M. Lou and H. Fang, "Deployment of Inflatable Space Structures:A Review of Recent Developments," *American Institute of Aeronautics and Astronautics* , vol. n.a, no. n.a, pp. 1-11, 2000.

[5] P. V. Cavallaro and A. M. Sadegh, "Air-Inflated Fabric Structures," in *Standard Handbook for Mechanical Engineers*, New York, McGraw-Hill, 2006, pp. 1-26.

[6] T. G. Priddy, "Inflatable Wing," United Sates Patent, Washington , 1988.

[7] A. Brown, "Inflatable Wing UAV Experimetal and Analytical Flight Mechanics," Georgia Institute of Technology , Georgia, 2011.

[8] D. Zizzo, "On a wing and some air: OSU Mars plane has inflatable wings," 13 February 2007. [Online]. Available: https://newsok.com/article/3012307/on-a-wing-and-some-airbrspan-classhl2osu-mars-plane-has-inflatable-wingsspan. [Accessed 17 January 2019].

[9] A. L. Dahir, "Kenya has legalized the commercial and private use of drones," 23 March 2018. [Online]. Available: https://qz.com/africa/1235759/kenya-legalized-drones-but-uber-and-facebook-didnt-apply-for-licenses/. [Accessed 17 January 2019].

[10] A. A. Bari, M. Mashud and H. Ali, "Role of Partially Bumpy Surface to Control the Flow Separation of an Airfoil," *ARPN Journal of Engineering and Applied Sciences* , vol. 7, no. 5, pp. 584-587, 2012.

[11] S. L. Veldman and C. A. J. R. Vermeeren, "Inflatable Structures in Aerospace Engineering - An Overview," in *European Conference on Spacecraft Structures, Materials and Mechanical Testing*, Noordwijk, 2000.

[12] T. Kinsey and G. Dumas, "Aerodynamics of Oscillating Wings and Performance as Wind Turbines," in *AIAA Applied Aerodynamics Conference*, Toronto, 2005.

[13] R. R. Harbig, J. Sheridan and M. C. Thompson, "Reynolds number and aspect ratio effects on the leading-edge vortex for rotating insect wing platforms," *Cambridge University Press*, vol. 717, no. 1, pp. 166 - 192, 2013.

[14] W. Commons, "NACA 4318," 23 July 2008. [Online]. Available: https://commons.wikimedia.org/wiki/File:NACA_4318.svg. [Accessed 22 April 2019].

Appendix

Appendix I: MATLAB Code for drawing the graph of lift and drag coefficient against angle attack as generated by X Foil at a Reynolds number of $138.6667 * 10^3$

```
%% Import the data
[~, ~, raw] = xlsread('C:\Users\Study\Desktop\Softwares\XFoil
P4\TEST4318.csv','TEST4318','A4:E10');
raw(cellfun(@(x) ~isempty(x) && isnumeric(x) && isnan(x),raw)) = {''};
% cellVectors = raw(:,[4,5]);
raw = raw(:,[1,2,3,4,5]);

%% Create output variable
data = reshape([raw{:}],size(raw));

%% Allocate imported array to column variable names
Angle_of_attack = data(:,1);
Lift_Coefficient_XFoil = data(:,2);
Drag_Coefficient_XFoil = data(:,4);

%% Clear temporary variables
clearvars data raw cellVectors;

yyaxis right
plot(Angle_of_attack,Lift_Coefficient_XFoil,'-.k*','LineWidth',3)
hold on
yyaxis left
plot(Angle_of_attack,Drag_Coefficient_XFoil,'-.b*','LineWidth',3)
hold off
xlabel('Angle of attack (°)','fontsize',15)
ylabel('Lift Coefficient XFoil & Drag Coefficient XFoil','fontsize',15)
legend('Drag Coefficient XFoil','Lift Coefficient XFoil','fontsize',1000)
```

Appendix II: MATLAB Code for drawing the graph of lift and drag Coefficient against varied Reynolds Numbers

```
%% Import the data
[~, ~, raw] = xlsread('C:\Users\Study\Desktop\Softwares\XFoil
P4\VELOCITY.csv','VELOCITY','A4:F11');
raw(cellfun(@(x) ~isempty(x) && isnumeric(x) && isnan(x),raw)) = {''};
% cellVectors = raw(:,[4,5]);
raw = raw(:,[1,2,3,4,5,6]);

%% Create output variable
data = reshape([raw{:}],size(raw));

%% Allocate imported array to column variable names
Reynolds_Number = data(:,2);
Lift_Coefficient_WindTunnel = data(:,5);
Drag_Coefficient_WindTunnel = data(:,6);


%% Clear temporary variables
clearvars data raw cellVectors;

yyaxis right
plot(Reynolds_Number,Lift_Coefficient_WindTunnel,'-.k*','LineWidth',3)
hold on
yyaxis left
plot(Reynolds_Number,Drag_Coefficient_WindTunnel,'-.b*','LineWidth',3)
hold off
xlabel('Reynolds number','fontsize',15)
ylabel('Lift Coefficient Wind Tunnel & Drag Coefficient Wind
Tunnel','fontsize',15)
legend('Lift Coefficient Wind Tunnel','Drag Coefficient Wind
Tunnel','fontsize',1000)
```

Appendix III: MATLAB Code for drawing the graph of lift and drag coefficient against angle attack as read from the Wind Tunnel at a Reynolds number of $138.6667 * 10^3$

```
%% Import the data
[~, ~, raw] = xlsread('C:\Users\Study\Desktop\Softwares\XFoil
P4\WINDTUNNEL.csv','WINDTUNNEL','A4:K10');
raw(cellfun(@(x) ~isempty(x) && isnumeric(x) && isnan(x),raw)) = {''};
% cellVectors = raw(:,[4,5]);
raw = raw(:,[1,2,3,4,5]);

%% Create output variable
data = reshape([raw{:}],size(raw));

%% Allocate imported array to column variable names
Angle_of_attack = data(:,1);
Lift_Coefficient_WindTunnel = data(:,3);
Drag_Coefficient_WindTunnel = data(:,5);

%% Clear temporary variables
clearvars data raw cellVectors;

yyaxis right
plot(Angle_of_attack,Lift_Coefficient_WindTunnel,'-.k*','LineWidth',3)
hold on
yyaxis left
plot(Angle_of_attack,Drag_Coefficient_WindTunnel,'-.b*','LineWidth',3)
hold off
xlabel('Angle of attack (°)','fontsize',15)
ylabel('Lift Coefficient Wind Tunnel & Drag Coefficient Wind
Tunnel','fontsize',15)
legend('Drag Coefficient Wind Tunnel','Lift Coefficient Wind
Tunnel','fontsize',1000)
```

Appendix IV: MATLAB Code for drawing the graph of lift coefficients from both X Foil and the wind tunnel against angle attack at a Reynolds number of $138.6667 * 10^3$

```
%% Import the data
[~, ~, raw] = xlsread('C:\Users\Study\Desktop\Softwares\XFoil
P4\COMBINED.csv','COMBINED','A2:E8');
raw(cellfun(@(x) ~isempty(x) && isnumeric(x) && isnan(x),raw)) = {''};
% cellVectors = raw(:,[4,5]);
raw = raw(:,[1,2,3,4,5]);

%% Create output variable
data = reshape([raw{:}],size(raw));

%% Allocate imported array to column variable names
Angle_of_attack = data(:,1);
Lift_Coefficient_XFoil = data(:,2);
Lift_Coefficient_Wind_Tunnel = data(:,4);

%% Clear temporary variables
clearvars data raw cellVectors;

yyaxis right
plot(Angle_of_attack,Lift_Coefficient_XFoil,'-.k*','LineWidth',3)
hold on
yyaxis left
plot(Angle_of_attack,Lift_Coefficient_Wind_Tunnel,'-.b*','LineWidth',3)
hold off
xlabel('Angle of attack (°)','fontsize',15)
ylabel('Lift Coefficient XFoil & Lift Coefficient Wind Tunnel','fontsize',15)
legend('Lift Coefficient Wind Tunnel','Lift Coefficient
XFoil','fontsize',1000)
```

Appendix V: MATLAB Code for drawing the graph of drag coefficients from both X Foil and the wind tunnel against angle attack at a Reynolds number of $138.6667 * 10^3$

```
%% Import the data
[~, ~, raw] = xlsread('C:\Users\Study\Desktop\Softwares\XFoil
P4\COMBINED.csv','COMBINED','A2:E8');
raw(cellfun(@(x) ~isempty(x) && isnumeric(x) && isnan(x),raw)) = {''};
% cellVectors = raw(:,[4,5]);
raw = raw(:,[1,2,3,4,5]);

%% Create output variable
data = reshape([raw{:}],size(raw));

%% Allocate imported array to column variable names
Angle_of_attack = data(:,1);
Drag_Coefficient_XFoil = data(:,3);
Drag_Coefficient_Wind_Tunnel = data(:,5);

%% Clear temporary variables
clearvars data raw cellVectors;

yyaxis right
plot(Angle_of_attack,Drag_Coefficient_XFoil,'-.k*','LineWidth',3)
hold on
yyaxis left
plot(Angle_of_attack,Drag_Coefficient_Wind_Tunnel,'-.b*','LineWidth',3)
hold off
xlabel('Angle of attack (°)','fontsize',15)
ylabel('Drag Coefficient XFoil & Drag Coefficient Wind Tunnel','fontsize',15)
legend('Drag Coefficient XFoil','Drag Coefficient Wind
Tunnel','fontsize',1000)
```